

Beamlines and Endstations

 [Printer-friendly version](#)  [PDF version](#)

Experimental stations at synchrotrons such as the Advanced Light Source (ALS) are known as endstations because they exist at the ends of beamlines. Several endstations are operated by CXRO, including the associated beamlines.

Beamline 6.1.2: Full-field Soft X-Ray Microscopy

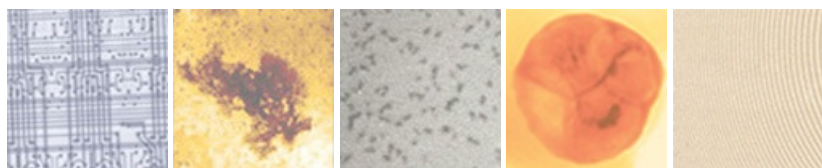
 [Printer-friendly version](#)  [PDF version](#)

The x-ray microscope XM-1 has been operational since 1994. It provides high spatial resolution (down to 15nm) imaging of samples which are transparent for soft X-rays. Its user-friendly design allows a high throughput of samples in a wide variety of applications such as nanomagnetism, materials and environmental science and biological applications. XM-1 is modeled after a conventional light microscope. The light we use is x-ray radiation emitted from a bending magnet, the lenses are zone plates, which are fabricated by the [Nanofabrication Laboratory of CXRO](#) and the image is formed onto a CCD detector. For more information, please see the [XM-1 site](#)

Science

 [Printer-friendly version](#)  [PDF version](#)

Research at XM-1



The current research activities utilize specific features of full-field soft X-ray transmission microscopy

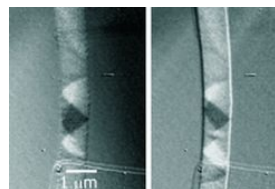
- elemental specificity of x-ray absorption
- high lateral resolution (currently down to 15nm) provided by Fresnel zone plates as optical elements
- large field of view of 15-20 μ m for a single image, which can be tiled up to even larger images
- recording images in varying external environments (magnetic fields, temperatures)
- sub-ns temporal resolution utilizing the pulsed time structure of the storage ring in a stroboscopic pump-probe scheme
- magnetic phase contrast imaging

Therefore XM-1 is used to image at high spatial and temporal [resolution](#) microscopic structures with applications to [magnetism](#), [materials](#) and [environmental](#) science and [biology](#).

Typical scientific topics include

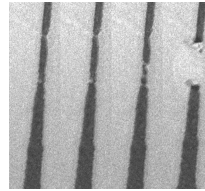
Magnetism

- spin current induced domain wall motion
- spin torque induced dynamics
- stochastic character of nucleation processes
- microscopic magnetization reversal behaviour in patterned media
- fast magnetization dynamics in patterned elements



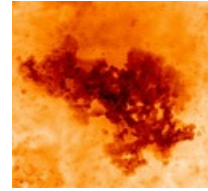
Materials science

- electromigration processes and void formation in interconnects



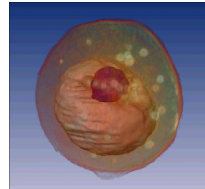
Environmental Science

- formation of cement



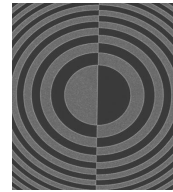
Biology

- imaging of Malaria infected blood cells
- 3D imaging of cell structures with x-ray tomography



Zone plate optics

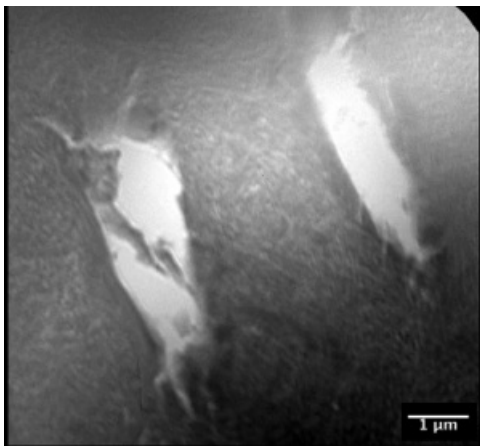
- phase sensitive Fourier optics
- development of preparation technique
- increasing the lateral resolution
- measuring zone plate efficiencies



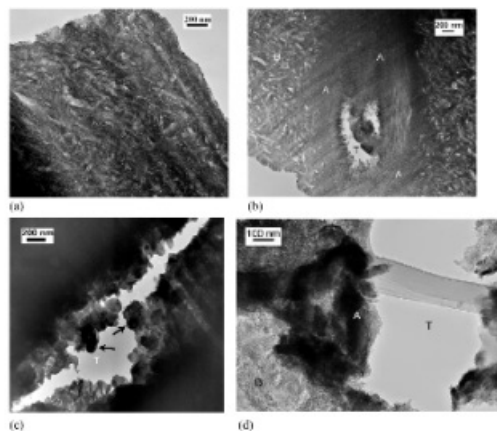
Material Sciences

 [Printer-friendly version](#)  [PDF version](#)

X-ray microscopy of mineralized tissues



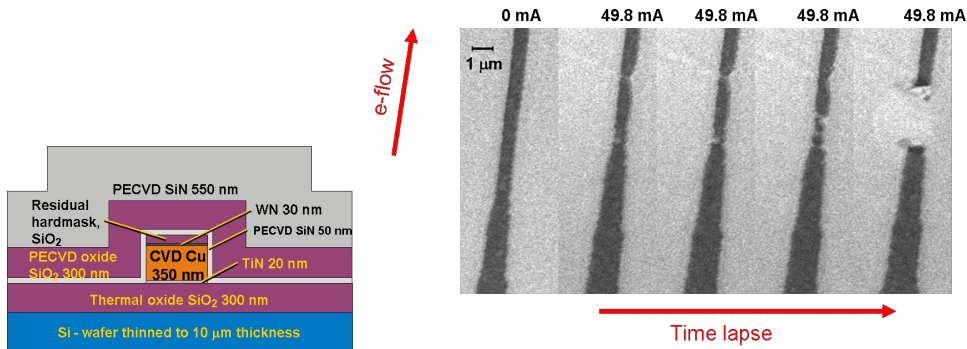
X-ray microscopy image of dentin sample recorded at $\lambda=2.4\text{nm}$ (516.6eV) with a MZP ($\Delta r_n=40\text{nm}$)



In comparison transmission electron micrographs of transparent dentin thinned using FIB-milling showing (a) intertubular dentin, (b) a partially filled tubule, (c) a tubule along its long axis partially filled with large mineral crystals, (d) the same sample as (a)-(c) prepared with ultramicrotome instead of FIB. (T= tubule, A= intratubular mineral, B= intertubular mineral) (courtesy J.W. Ager, LBNL (2006))

In Situ Studies of the Electromigration in Cu Interconnects

Recent experiments at XM-1 demonstrated that a full-field transmission x-ray microscope, operating at 1.8 keV photon energies, allows detection of passivated interconnects made from Cu or AlCu as well as vias utilizing the high material contrast from different elements in such integrated circuits with a resolution of about 40 nm. The mass flow caused by electromigration in a passivated Cu interconnect was studied in-situ at current densities up to 10^7 A/cm².



G. Schneider, M.A. Meyer, G. Denbeaux, et al., *Journal of Vacuum Science and Technology B*, 20, 3089 (2002)

Environmental Science

[Printer-friendly version](#) [PDF version](#)

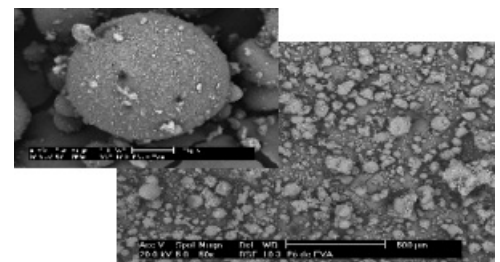
Insight into the Hydration Evolution of Cement

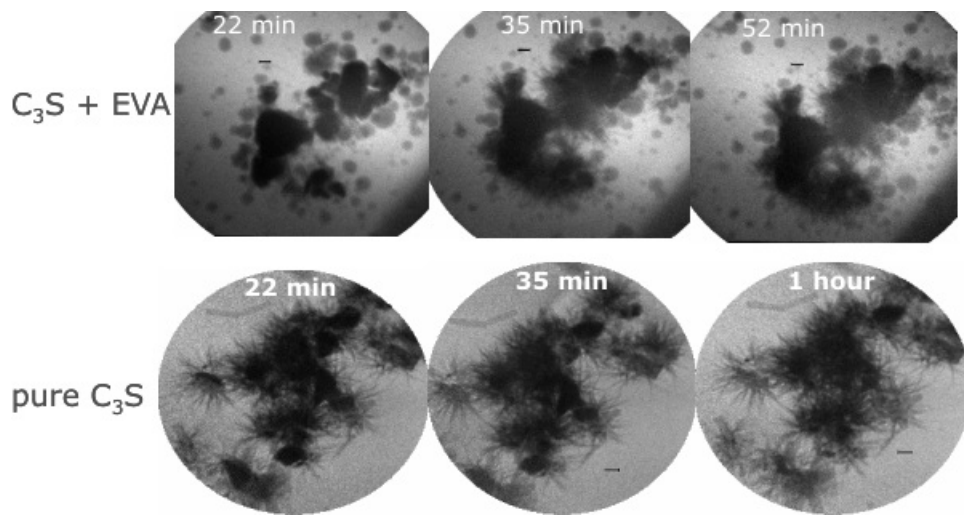


- sample is sandwiched between two Si₃N₄ windows
- highly diluted samples (ratio water/cement is 5 before centrifugation)
- Imaging starts within 6 minutes after mixing, under atmospheric pressure and room temperature
- evolution is followed for several hours



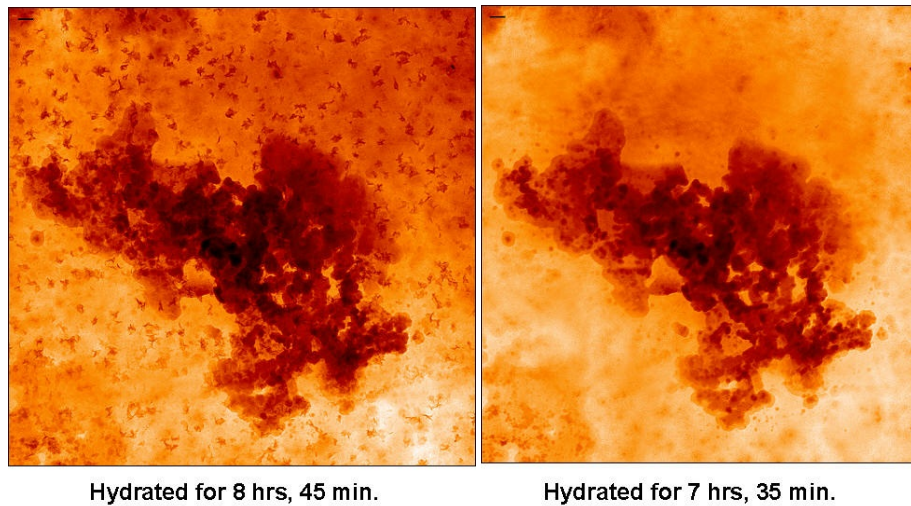
C3S (tricalcium silicate) - **EVA** (poly(ethylene-co-vinyl acetate) composites





D.A. Silva and P.J.M. Monteiro, Cement and Concrete Research 35(10) (2005) 2026-2032

High resolution time lapse images of the hydration of Calcium Aluminate cement



D.A. Silva and P.J.M. Monteiro, Cement and Concrete Research 35(10) (2005) 2026-2032

Biological Imaging

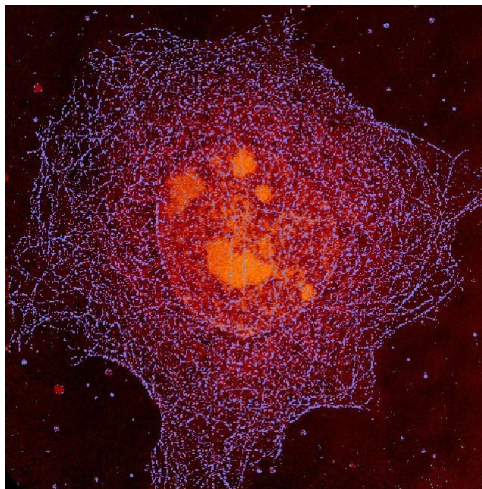
[Printer-friendly version](#) [PDF version](#)

The majority of biological x-ray microscopy studies are done in the water window, which is for photon energies between the K shell absorption edges of Oxygen (543 eV, 2.3 nm) and Carbon (284 eV, 4.4 nm). For x-ray energies just below the Oxygen edge (e.g., 517 eV, 2.4 nm), the absorption of mostly carbon-containing organic material is about an order of magnitude less than the absorption of water, permitting a natural contrast. The penetration depth of these soft x-rays is also ideally suited to image intact

cells with a thickness of a few microns. The photoelectric absorption, which provides contrast in soft x-ray microscopy, is also responsible for significant radiation damage to biological samples. However, it is possible to prepare samples in different stages of development and then make conclusions based on statistical methods; a common method used with electron microscopy.

Cells which are sensitive to radiation damage can be chemically fixed to maintain cell structure during x-ray imaging. In addition, a labeling technique for localizing specific proteins within cellular structure can be used. Natural antibodies are utilized to attach dense silver and gold particles to the protein of interest. A computerized process is used after the imaging to locate the sharp increases in intensity to identify the regions of labeling.

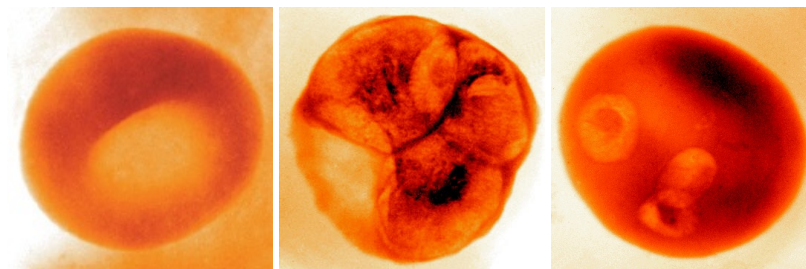
For other types of experiments, we have a sample holder for imaging cryogenically frozen cells, which mitigates the effects of radiation damage. Because of this, chemical fixation is not needed, which results in images with remarkable detail.



Tubulin Network in Epithelial Cell

W. Meyer-Ilse, A. Nair/ CXRO

C. Larabell, S. Lelièvre, D. Hamamoto, M. Bissell / Life Sciences Division



*X-ray images of malaria infected blood cells obtained at 2.4nm wavelength.
Left: uninfected cell, Center: newly infected cell, Right: cell 36h after infection.*

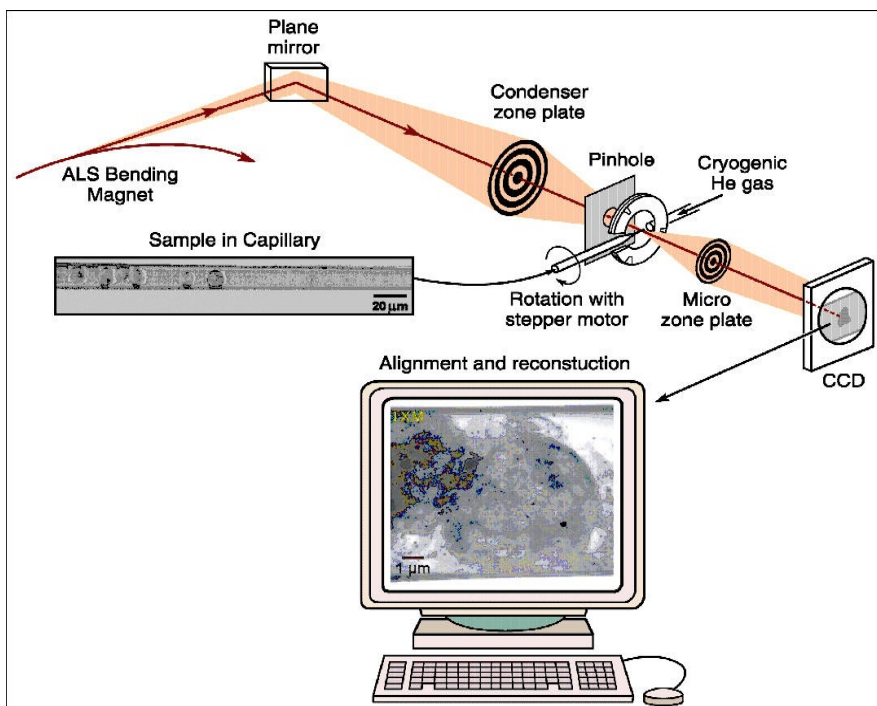
C. Magowan, W. Meyer-Ilse and J. Brown, LBNL

Recording a series of images of a specimen mounted in a rotational stage with the rotation axis perpendicular to the photon beam direction opens the avenue for X-ray tomography at high lateral resolution to study 3-dim structures in cells. A new X-ray microscope is currently being set-up by the National Center for X-ray tomography at the ALS.

X-Ray Tomography

 [Printer-friendly version](#)  [PDF version](#)

To determine 3D structures with high lateral resolution one can record a series of X-ray images with the sample mounted into a rotating stage. Each image represents the 2D projection of the structures as viewed at different rotation angles which can be reconstructed in the computer to give the full 3D information.

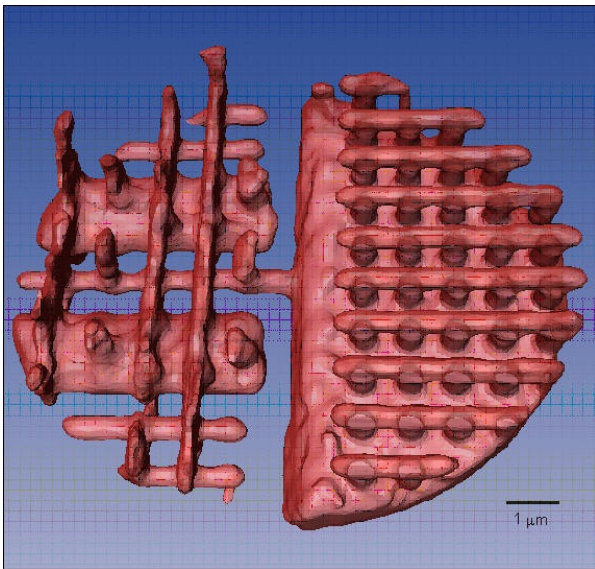


Bio-nanotomography of Yeast Cells

[Launch
in external player](#)

courtesy: C. Larabell and M. LeGros, LBNL and UC San Francisco

X-ray tomography of Cu interconnects

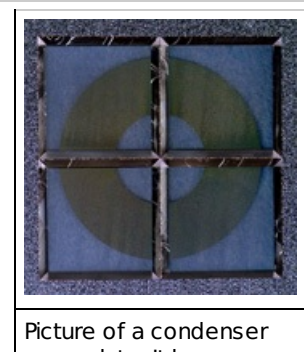
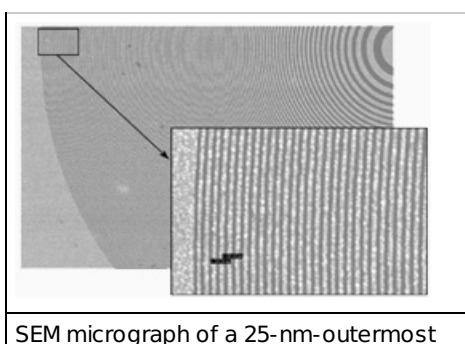
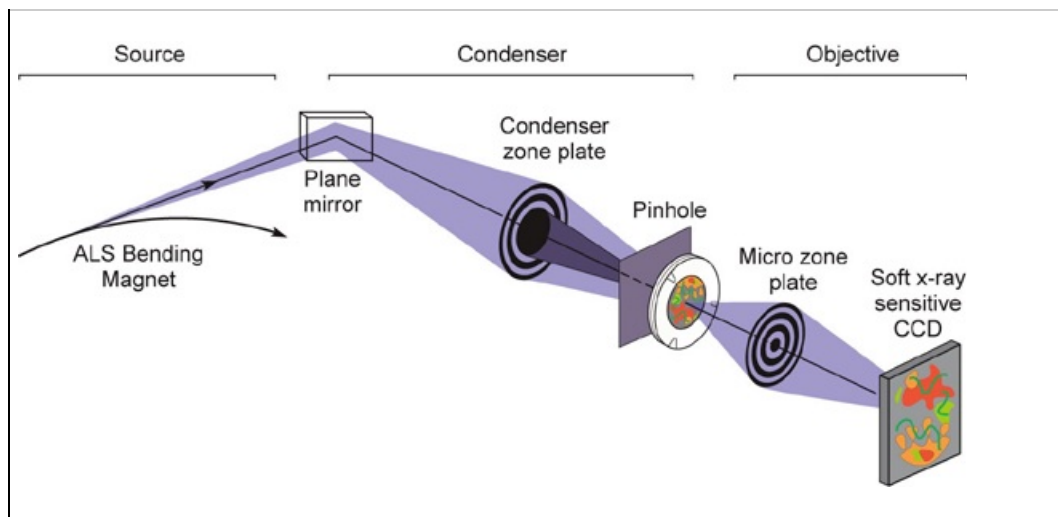


Rendered image after tomographic reconstruction of 50 images over 140 degrees
 courtesy: G. Schneider, M.A.Meyer, G.Denbeaux et al; BESSY, Germany [*Applied Physics Letters*, 81(14), 2002]

Resolution

[Printer-friendly version](#) [PDF version](#)

Fresnel zone plates are used in the microscope as condenser (condenser zone plate) and imaging (micro zone plate) optics. They are fabricated in-house using the Nanowriter electron beam lithography tool in the [Nanofabrication Laboratory](#).



zone width micro zone plate. Diameter = 63mm, 628 zones, gold plated

zone plate. It has an outermost zone width of 60 nm, 41700 zones, 1 cm diameter, and nickel plating.

Characterization of the spatial resolution of the microscope is an important and active project in our group. Here, we use the following definition of resolution:

Res = half-period of a equal line and space pattern that exhibits Rayleigh-like 26.5% modulation in its image

The resolution, in general, can be expressed as $k_1 \lambda / NA$. λ is the radiation wavelength, and NA is the numerical aperture of the imaging optic. k_1 is a constant which primarily depends on the degree of partial coherence of the illumination, σ . In our case, NA is equal to $\lambda / (2\Delta r_{M2P})$, where $2\Delta r_{M2P}$ is the outermost zone width of the micro zone plate. Thus,

$$Res = 2 k_1 \Delta r_{M2P}$$

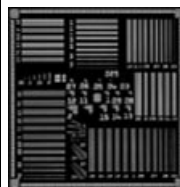
The degree of partial coherence of the microscope, σ , is equal to $NA_{condenser} / NA_{imaging} = \Delta r_{M2P} / \Delta r_{CZP}$. Δr_{CZP} is the outermost zone width of the condenser zone plate (CZP). Typically, σ is from 0.4 to 0.7, and k_1 from 0.6 to 0.8. The resolution of the full-field microscope is slightly finer than the smallest zone width of the micro zone plate.

We design and fabricate various test objects for measurement of the microscope's resolution. Test objects and measurement result are discussed below.

Recent Results [\(Click for Larger Images\)](#)

Resolution Test Object

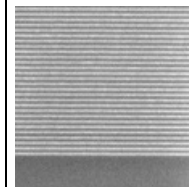
- Fabricated in-house using Nanowriter electron beam lithography
- Flexible, arbitrary, 2-D line and space patterns
- Features as fine as the smallest zones in the zone plates
- Typical in gold or nickel plating on silicon nitride window



Design layout of a test object. The numbers represent linewidth in microns.

Multilayer Test Object

- Multilayer coatings in cross section
- Fabricated in-house using magnetron sputtering and conventional TEM sample preparation techniques
- high quality layers with halfperiods down to 5 nm
- large material pair selections
- arbitrary aspect ratio



SEM micrograph of Cr/Si test object

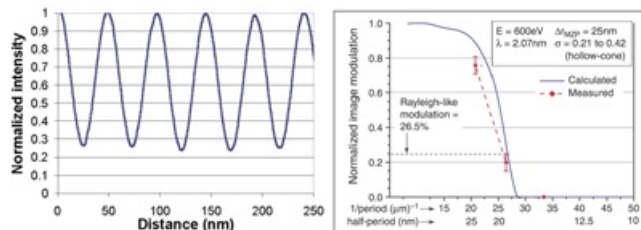
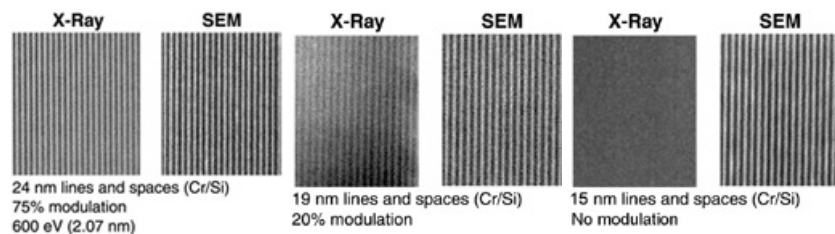
Resolution Measurement

20 nm spatial resolution in 1.1x diffraction limit at 2.07 nm

Achieved with a 25-nm outermost zone width micro zone plate, and $s = 0.42$

$\Delta r_{M2P} = 25 \text{ nm}$, $D = 30 \text{ }\mu\text{m}$, $N = 300$, $\sigma = 0.42$
 $\Delta r_{CZP} = 60 \text{ nm}$, diameter = 10 mm, $N = 41700$

[Click for Larger Images](#)



People at XM-1

[Printer-friendly version](#) [PDF version](#)

People at XM-1



Peter Fischer



Dong-Hyun Kim



Brooke Mesler



Weilun Chao



Anne Sakdinawat



Bob Gunion



Ron Oort



Drew Kemp



Seno Rekawa



Paul Denham



Kevin Bradley



David Attwood

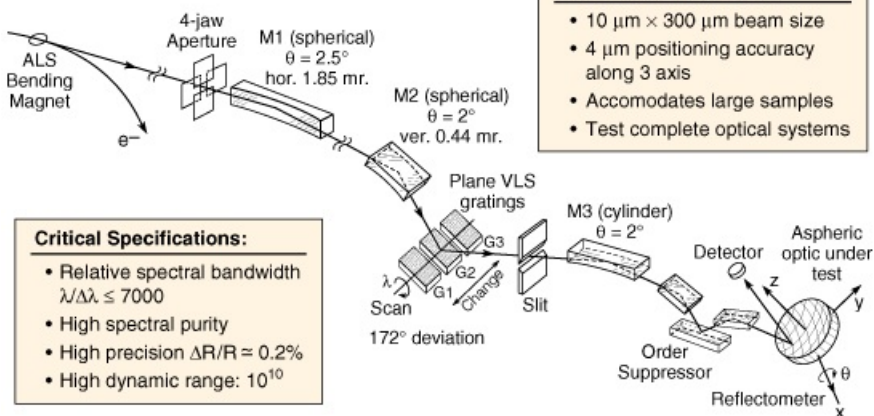


Erik Anderson

Beamline 6.3.2: EUV and Soft X-Ray Reflectometry and Scattering

[Printer-friendly version](#) [PDF version](#)

50-1300 eV energy range



Beamline 6.3.2 is a PRT-owned bend magnet beamline dedicated to EUV and soft x-ray reflectometry and scattering. The beamline, in operation since February 1995, is designed for high spectral purity and wavelength accuracy. Owned by the Berkeley Labs Center for X-ray Optics, the beamline is used for the characterization of optical components and reflective coatings for a variety of applications including EUV lithography.

High spectral resolution is obtained using a variable-line spaced plane grating monochromator. The monochromator, designed and constructed by the Center for X-ray Optics, uses no entrance slit and a fixed exit slit. The light is focussed onto the sample by the first horizontally deflecting mirror and a bendable refocusing mirror downstream from the monochromator. High spectral purity is achieved using a combination of filters and a triple mirror "order-suppressor".

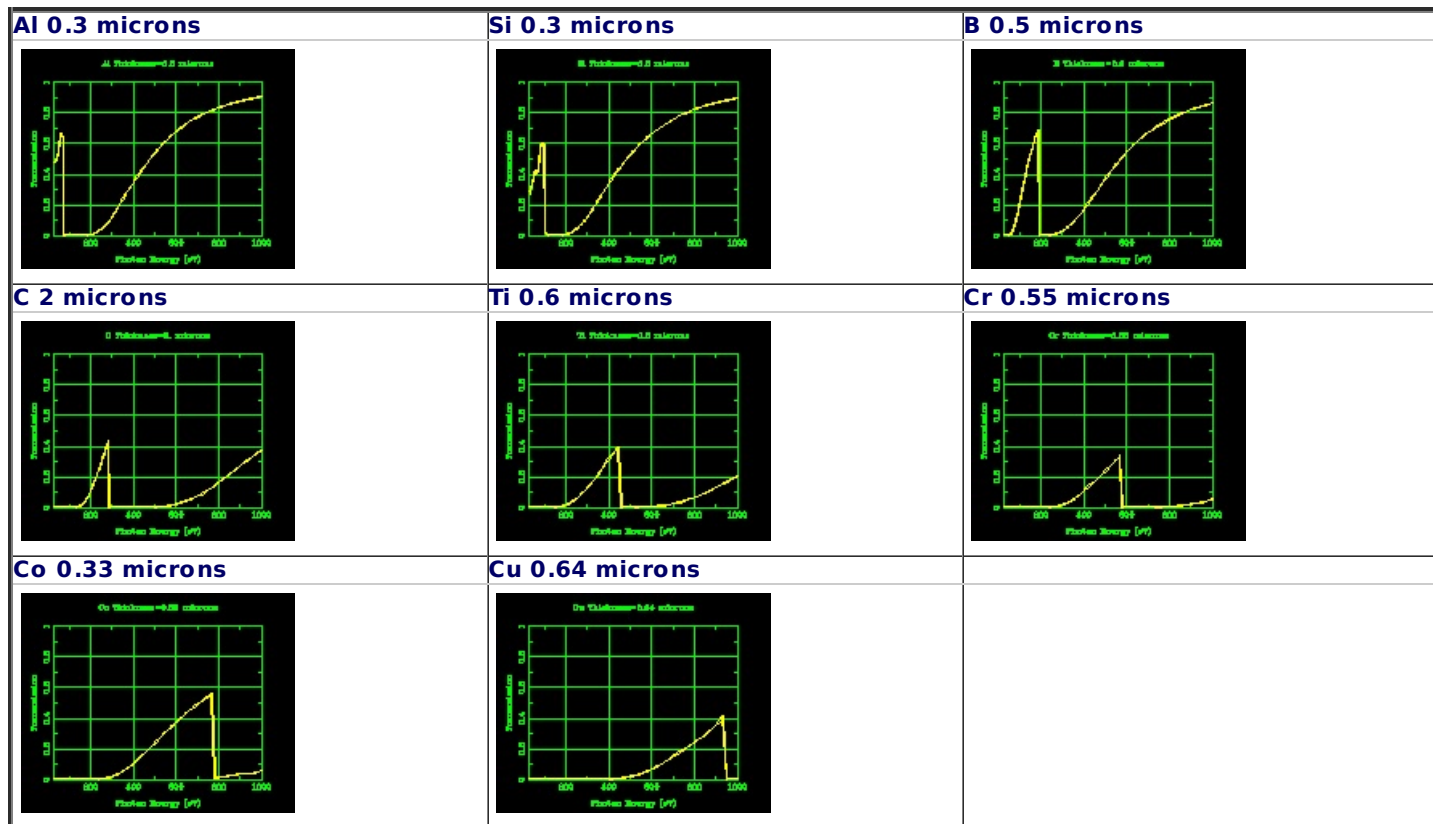
A permanent reflectometer end-station is available. A sample may be positioned in three dimensions to a precision of 4 microns. Samples of up to 8 inches in diameter may be accommodated. An array of detectors including a photodiode, channeltron and CCD camera are mounted on a rotating arm. Space is available for additional endstations downstream from the reflectometer.

For more information on beamline 6.3.2, please contact: [EMGullikson \[at\] lbl \[dot\] gov](mailto:EMGullikson@lbl.gov)

View the [beamline schedule in an Excel spreadsheet](#).

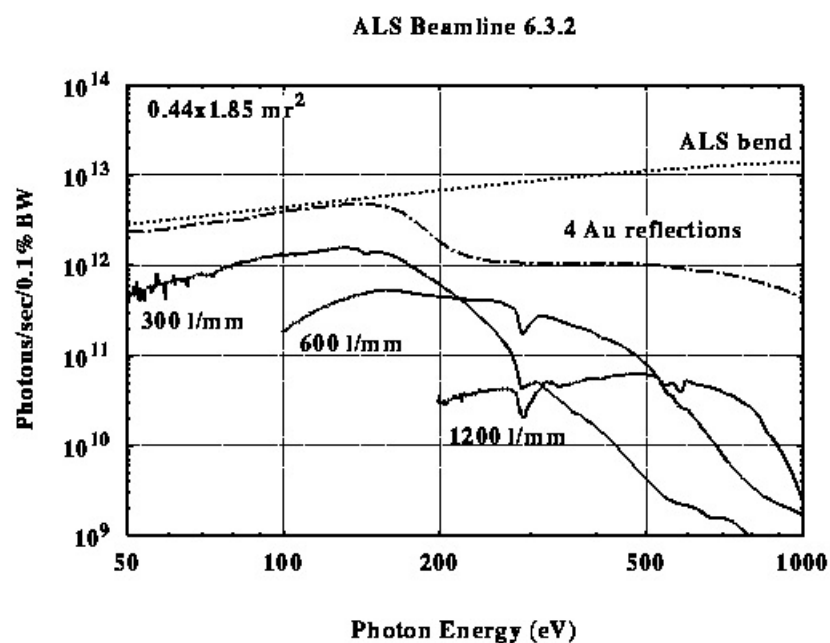
Beamline 6.3.2 Filters

[Printer-friendly version](#) [PDF version](#)



Beamline 6.3.2 Flux

[Printer-friendly version](#) [PDF version](#)

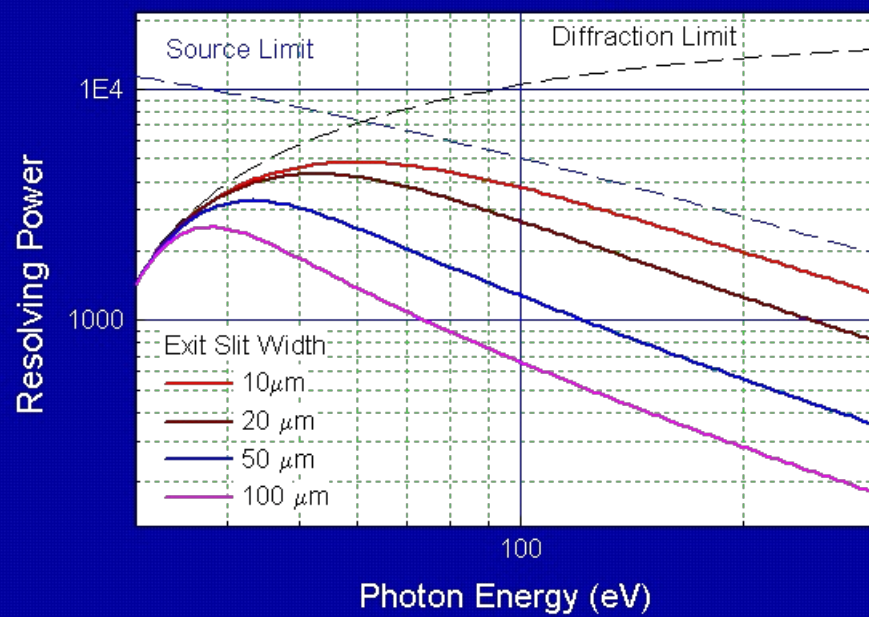


Beamline 6.3.2 Monochromator Resolution

[Printer-friendly version](#) [PDF version](#)

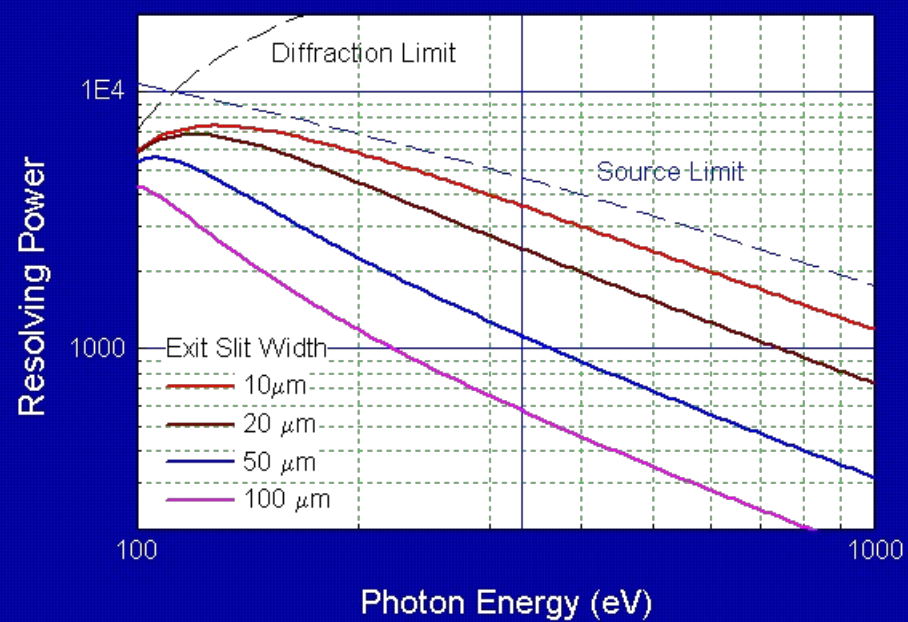
1

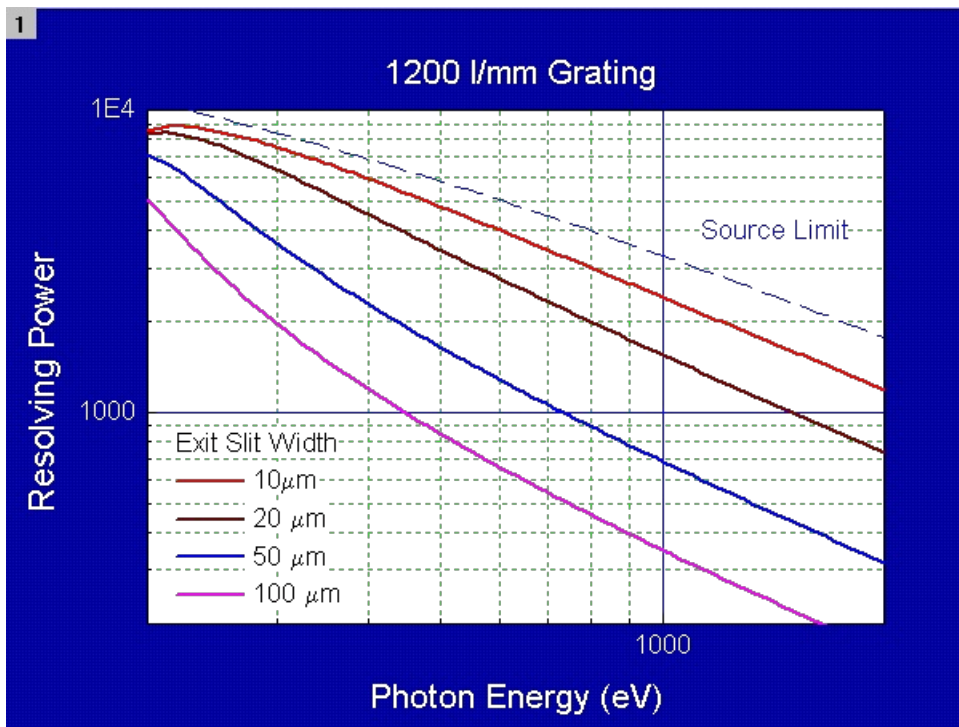
200 l/mm Grating



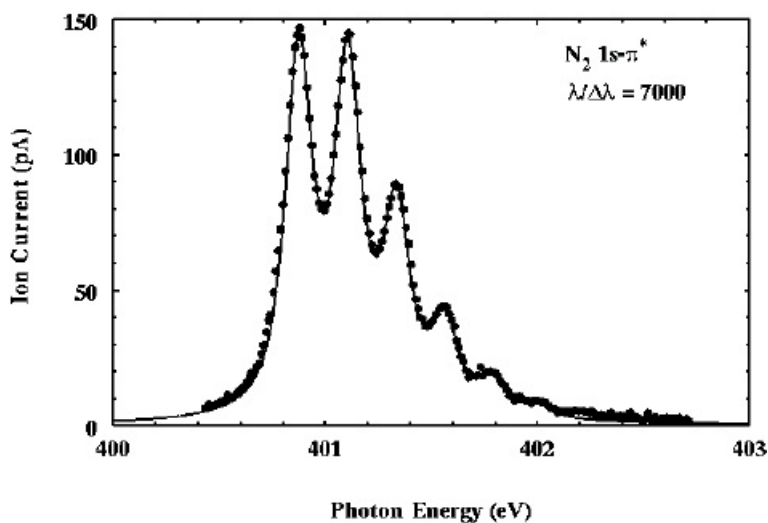
1

600 l/mm Grating





N2 Absorption Spectrum Illustrating the High Resolution



Beamline 11.3.2: EUV Mask Inspection

[Printer-friendly version](#) [PDF version](#)

In Photolithography, masks carry the pattern that is transferred onto a wafer.

Any printable defect can spoil the die.



Extreme Ultraviolet (EUV) lithography relies on multilayer-coated mirrors and 13-nm-wavelength light. An EUV mask, or reticle, is made from a nearly perfect mirror coated with a patterned absorber layer. A mask is a highly complex optical system made from more than five different materials. The structure and material properties give the mask a wavelength-specific response and make testing with EUV light essential during development.

We have created a world-leading high-resolution EUV microscope capable of measuring the reflective properties of a mask on a 100-nm length scale, or smaller. Working in close collaboration with semiconductor industry sponsors, the project's goals include:

1. Understand and quantify EUV defects and repair strategies
2. Qualify other inspection tools becoming available world-wide
3. Validate and improve modeling
4. Evaluate the performance of actinic inspection



For more information, please visit [the mask inspection site](#).

Beamline 12.0.1: EUV Interferometry

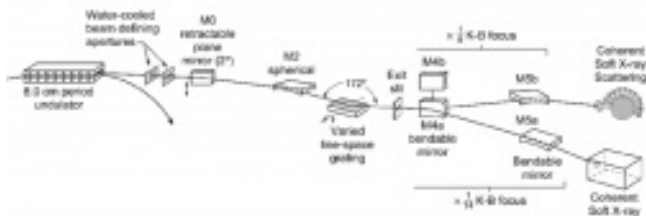
 [Printer-friendly version](#)  [PDF version](#)

Beamline 12.0.1 provides an endstation for [EUV Lithography](#) which is heavily used by many industrial partners in the semiconductor industry.

Beamline 12.0.2.1: Coherent Soft X-Rays

 [Printer-friendly version](#)  [PDF version](#)

Beamline 12.0.2.1 provides tunable, spatially and spectrally coherent soft X-ray radiation for the purposes of characterizing novel x-ray optics. Using the third harmonic from an 8-cm period undulator, this branch delivers coherent soft X-rays with photon energies ranging from 200 to 1000 eV. The layout of the beamline is depicted below. The branchline consists of four mirrors and a monochromator. The first optic is a 2 horizontally deflecting planar mirror coated in gold which deflects the beam into beamline 12.0.2. The next is a spherical vertically deflecting mirror coated in iridium that focuses the source onto the exit slit. Next along the beam path is the monochromator composed of a varied line-space grating and an exit slit, enabling a bandwidth of as low as 0.1%. Lastly are two pairs of tungsten coated mirrors comprising the Kirkpatrick-Baez focus system for the two subbranches, one at 14 demagnification and the other 8 demagnification. The former is optimized for use at 500 eV and the latter at 800 eV. In each subbranch demagnification is equivalent in the horizontal and vertical directions.



Beamline 12.0.2.1 layout, from [1]. Click on the image to see the full size version. For further information please see the [diffractive optics](#) page and the [publications](#) list. [1] *Tunable coherent soft X-rays* Rosfjord, K.M.; Yanwei Liu; Attwood, D.T.; *Selected Topics in Quantum Electronics, IEEE Journal of Volume 10, Issue 6, Nov-Dec 2004 Page(s):1405 - 1413*